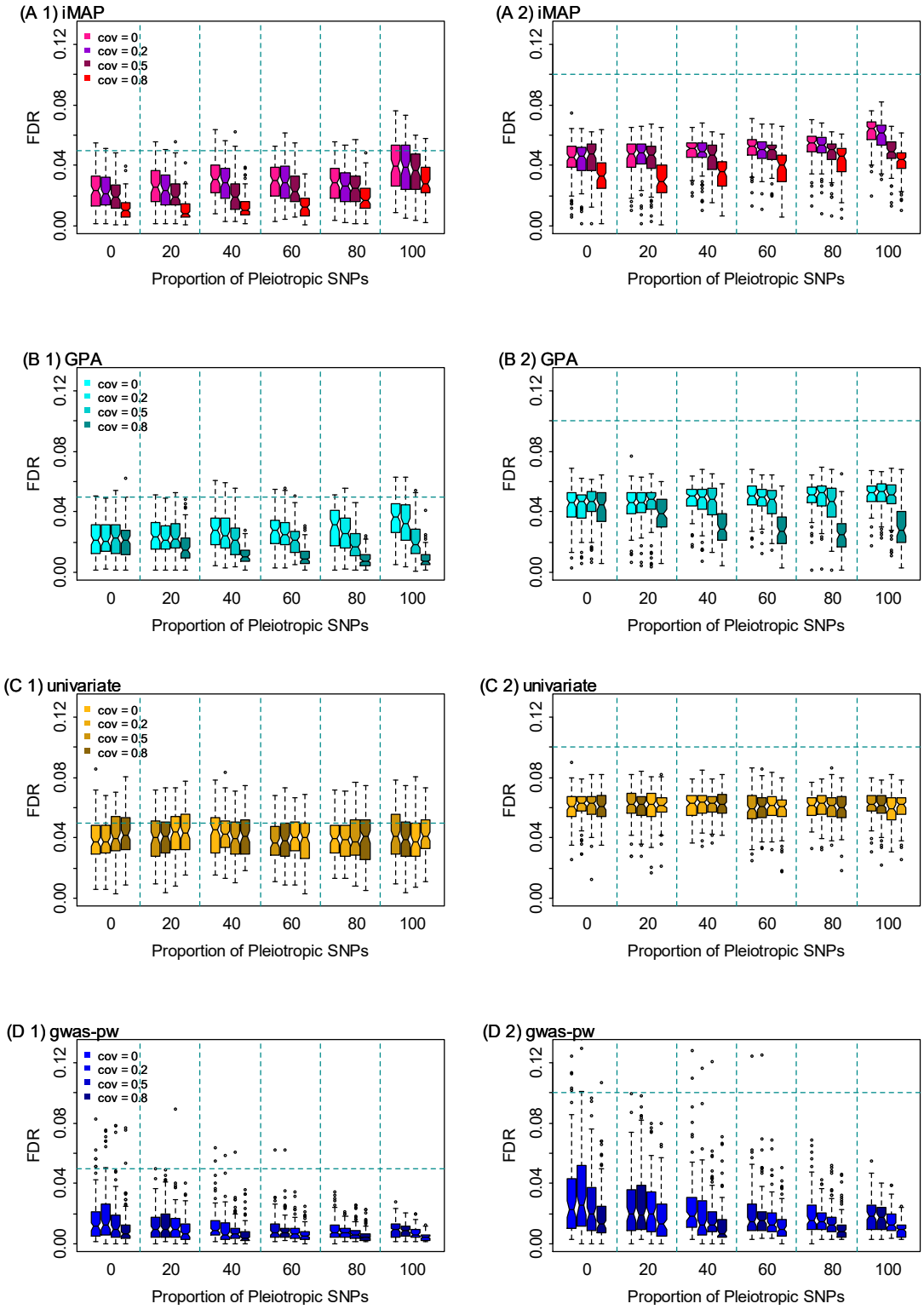

Fig. S1. False discovery rate (FDR) control by various methods in the simulation setting where the two traits are positively correlated. Estimated FDR (y-axis) by (A)

iMAP, (B) GPA, (C) univariate analysis, and (D) gwas-pw, in settings where the proportion of pleiotropic causal SNPs varies from 0% to 100% (x-axis). In each line the first and the second plots correspond to the true FDR value of 0.05 and 0.10, respectively.

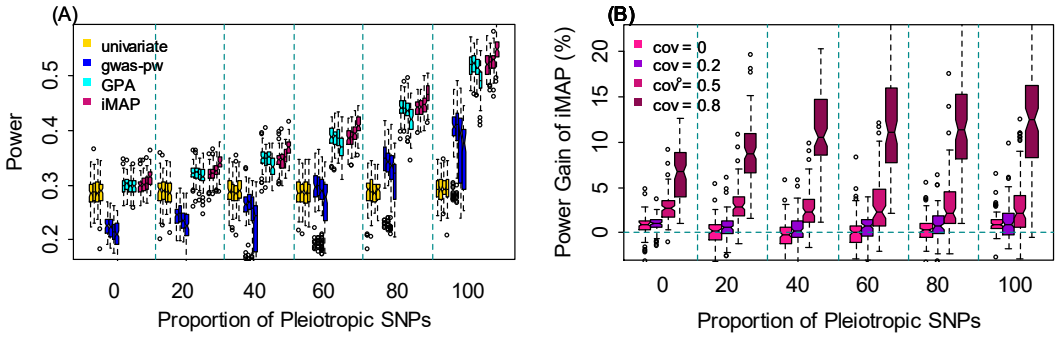

Fig. S2. Comparison of power in detecting associated SNPs by various methods in the simulation setting where the two traits are positively correlated. Methods for comparison include univariate analysis, gwas-pw, GPA and iMAP. (A) Power (y-axis) is measured at a fixed false discovery rate (FDR) of 0.10, in settings where the proportion of pleiotropic causal SNPs varies from 0% to 100% (x-axis). For each method, the four boxplots at each pleiotropic proportion level correspond to four different phenotypic covariance values of 0, 0.2, 0.5 and 0.8, respectively. (B) Power gain of iMAP with respect to GPA computed based on panel (A).

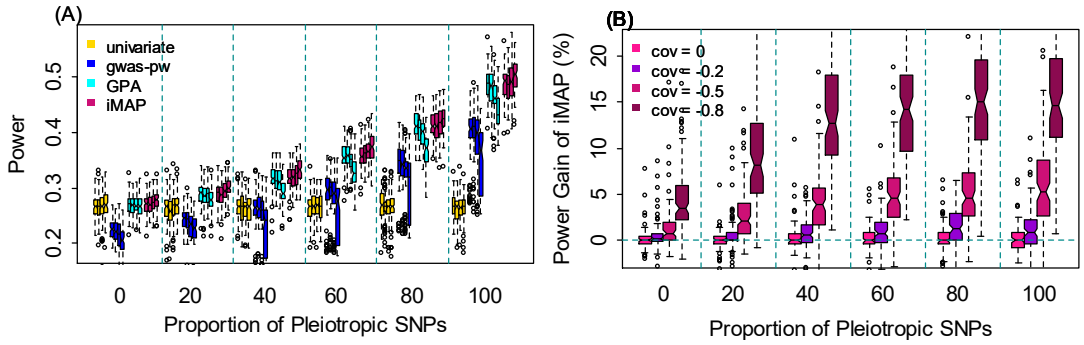

Fig. S3. Comparison of power in detecting associated SNPs by various methods in the simulation setting where the two traits are negatively correlated. Methods for comparison include univariate analysis, gwas-pw, GPA and iMAP. (A) Power (y-axis) is measured at a fixed false discovery rate (FDR) of 0.05, in settings where the proportion of pleiotropic causal SNPs varies from 0% to 100% (x-axis). For each method, the four boxplots at each pleiotropic proportion level correspond to four different phenotypic covariance values of 0, -0.2, -0.5 and -0.8, respectively. (B) Power gain of iMAP with respect to GPA computed based on panel (A).

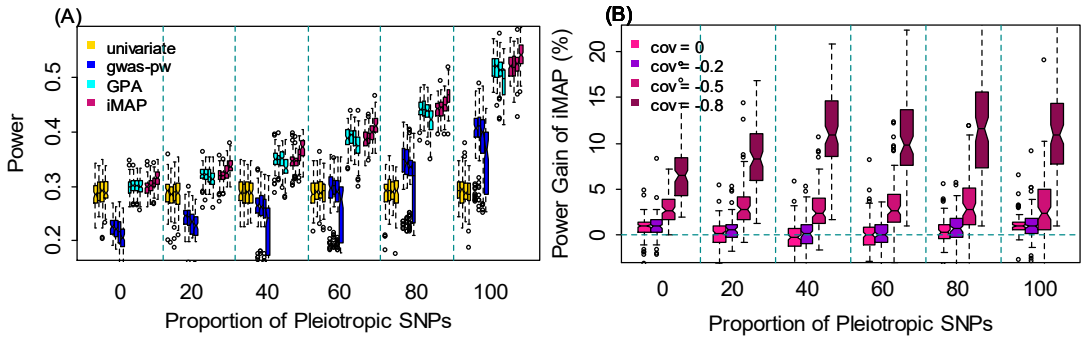

Fig. S4. Comparison of power in detecting associated SNPs by various methods in the simulation setting where the two traits are negatively correlated. Methods for comparison include univariate analysis, gwas-pw, GPA and iMAP. (A) Power (y-axis) is measured at a fixed false discovery rate (FDR) of 0.10, in settings where the proportion of pleiotropic causal SNPs varies from 0% to 100% (x-axis). For each method, the four boxplots at each pleiotropic proportion level correspond to four different phenotypic covariance values of 0, -0.2, -0.5 and -0.8, respectively. (B) Power gain of iMAP with respect to GPA computed based on panel (A).

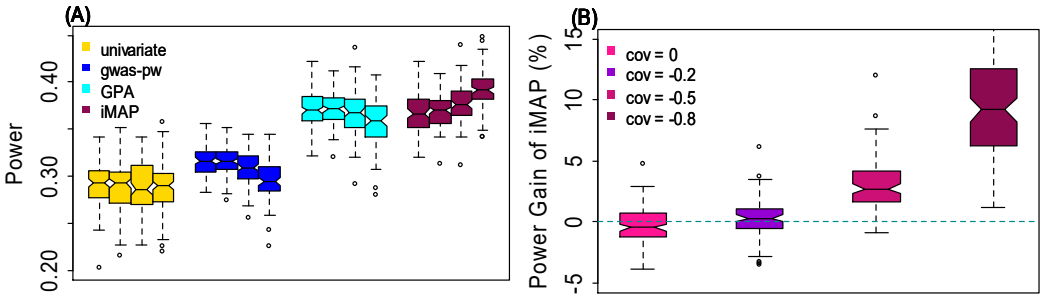

Fig. S5. Comparison of power in detecting associated SNPs by various methods in the simulation setting where the two traits are positively correlated. Methods for comparison include univariate analysis, gwas-pw, GPA and iMAP. (A) Power (y-axis) is measured at a fixed false discovery rate (FDR) of 0.05. For each method, the four boxplots correspond to four different phenotypic covariance values (x-axis) of 0, 0.2, 0.5 and 0.8, respectively. (B) Power gain of iMAP with respect to GPA computed based on panel (A). In this simulation setting, SNPs were divided into 500 equal-size regions, among which about 60% (i.e. the pleiotropic proportion) were causal; in each causal region, two causal SNPs were randomly selected to be related to only the first trait, or the second trait, or both traits.

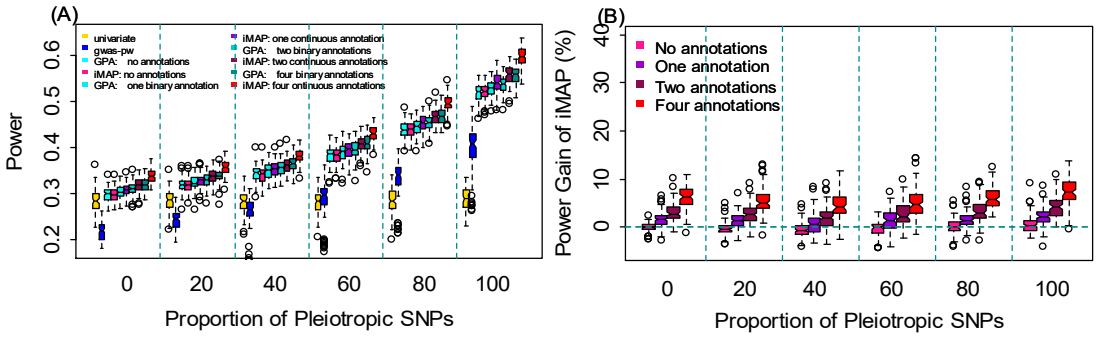

Fig. S6. Comparison of power in detecting associated SNPs by various methods in the presence of informative annotations. Methods for comparison include univariate analysis, gwas-pw, GPA and iMAP. Variations of GPA and iMAP that incorporate a different number of annotations (0, 1, 2 and 4) are considered. iMAP uses the original continuous annotations while GPA has to rely on the dichotomized annotations. (A) Power (y-axis) is measured at a fixed false discovery rate (FDR) of 0.10, in settings where the proportion of pleiotropic causal SNPs varies from 0% to 100% (x-axis). (B) Power gain of iMAP with respect to GPA computed based on panel (A).

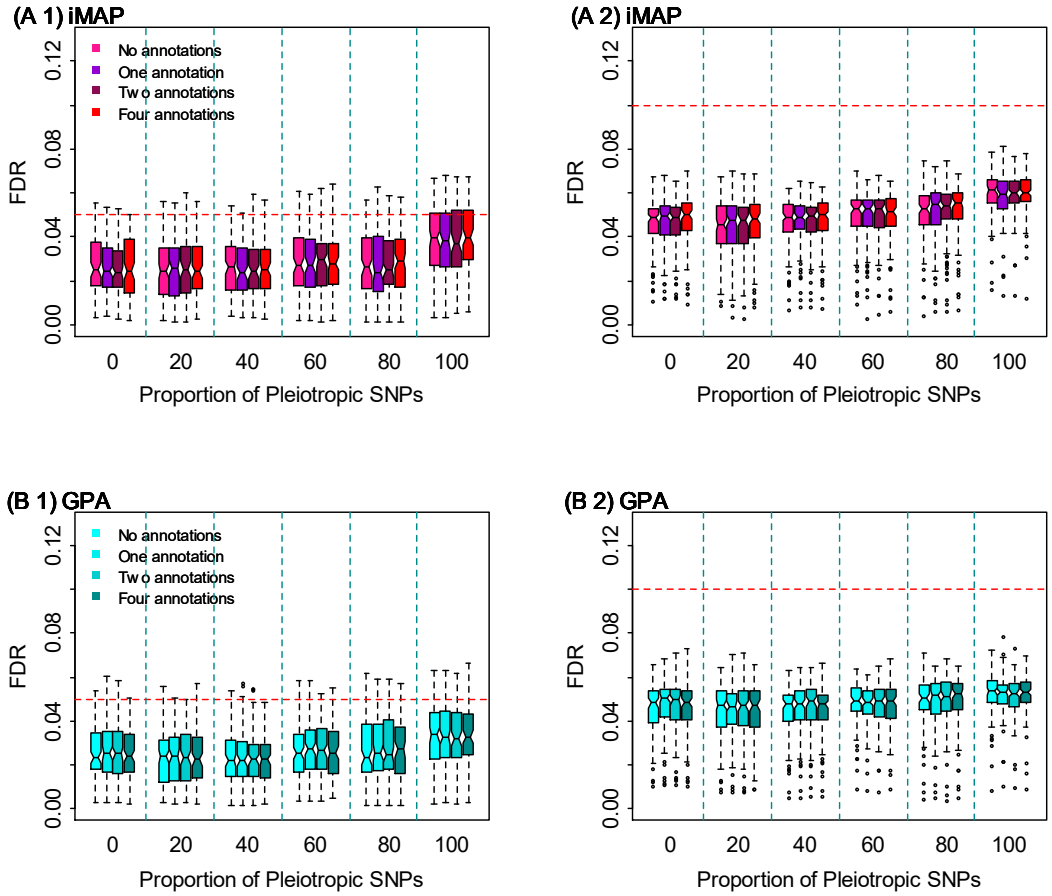

Fig. S7. False discovery rate (FDR) control by various methods in the presence of informative annotations. Estimated FDR (y-axis) by (A) iMAP and (B) GPA at the true FDR of 0.05 (the first plot in the panel) and 0.10 (the second plot in the panel), in settings where the proportion of pleiotropic causal SNPs varies from 0% to 100% (x-axis). Variations of GPA and iMAP that incorporate a different number of annotations (0, 1, 2 or 4) are considered.

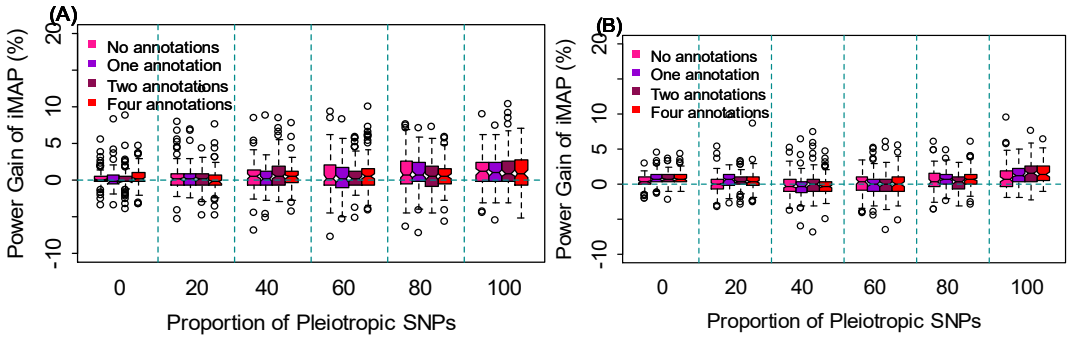

Fig. S8. Comparison of power in detecting associated SNPs by various methods in the presence of informative annotations. Both iMAP and GPA use the dichotomized annotations here. (A) Power gain (y-axis) of iMAP with respect to GPA at a fixed false discovery rate (FDR) of 0.05, in settings where the proportion of pleiotropic causal SNPs varies from 0% to 100% (x-axis). (B) Power gain (y-axis) of iMAP with respect to GPA at a fixed false discovery rate (FDR) of 0.10.

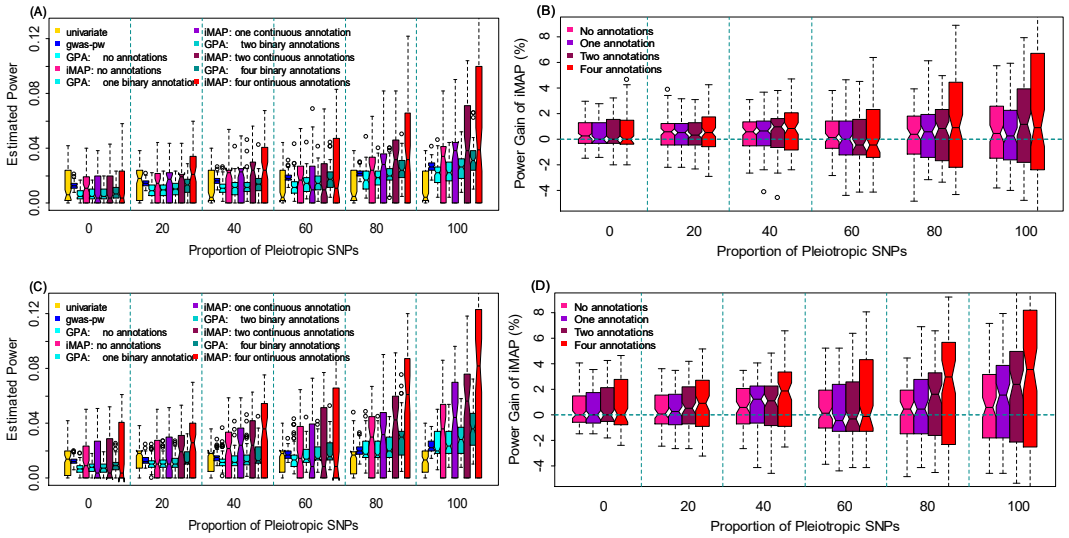

Fig. S9. Comparison of power in detecting associated SNPs by various methods in the presence of informative annotations. Methods for comparison include univariate analysis, gwas-pw, GPA and iMAP. Here the proportion of phenotypic variance explained (PVE) by all causal SNPs was set to 0.20. Variations of GPA and iMAP that incorporate a different number of annotations (0, 1, 2 and 4) are considered. iMAP uses the original continuous annotations while GPA has to rely on the dichotomized annotations. (A) Power (y-axis) is measured at a fixed false discovery rate (FDR) of 0.05, in settings where the proportion of pleiotropic causal SNPs varies from 0% to 100% (x-axis). (B) Power gain of iMAP with respect to GPA computed based on panel (A). (C) Power (y-axis) is measured at a fixed false discovery rate (FDR) of 0.10, in settings where the proportion of pleiotropic causal SNPs varies from 0% to 100% (x-axis). (D) Power gain of iMAP with respect to GPA computed based on panel (C).

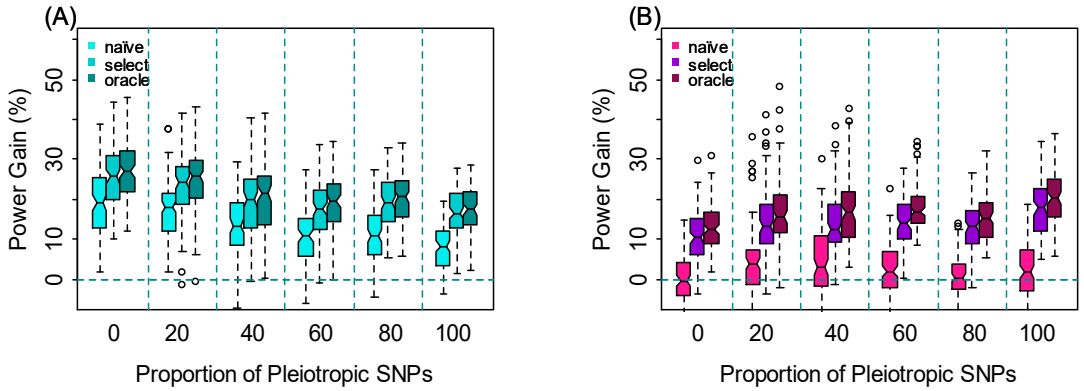

Fig. S10. Power comparison between different variations of GPA and iMAP in the presence of four informative annotations and 100 noninformative annotations. Different variations of GPA and iMAP are considered: the naïve version does not incorporate any annotations; the full version includes all the annotations; the select version performs annotation selection; and the oracle version uses the four informative annotations. (A) Power gain of GPA-naïve, GPA-select and GPA-oracle over GPA-full. (B) Power gain of iMAP-naïve, iMAP-select and iMAP-oracle over iMAP-full.

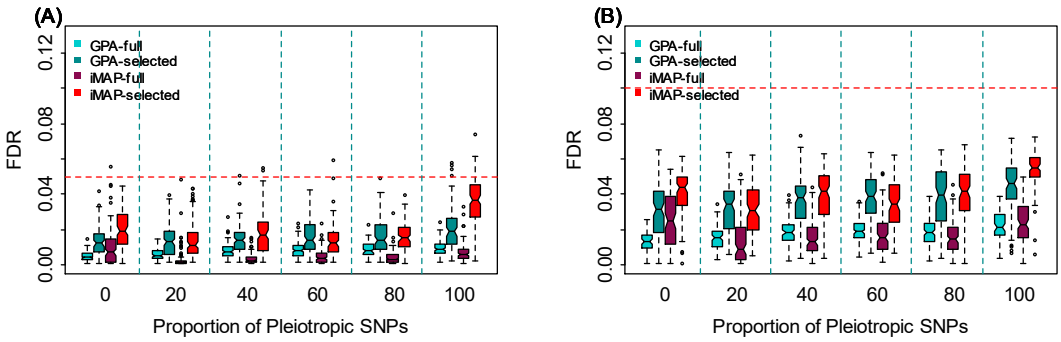

Fig. S11. False discovery rate (FDR) control by iMAP and GPA in the presence of four informative annotations and 100 non-informative annotations. Two variations of GPA and iMAP are considered: the full version includes all the annotations, while the select version performs annotation selection. (A) FDR control corresponds to the true value of 0.05; (B) FDR control corresponds to the true value of 0.10.

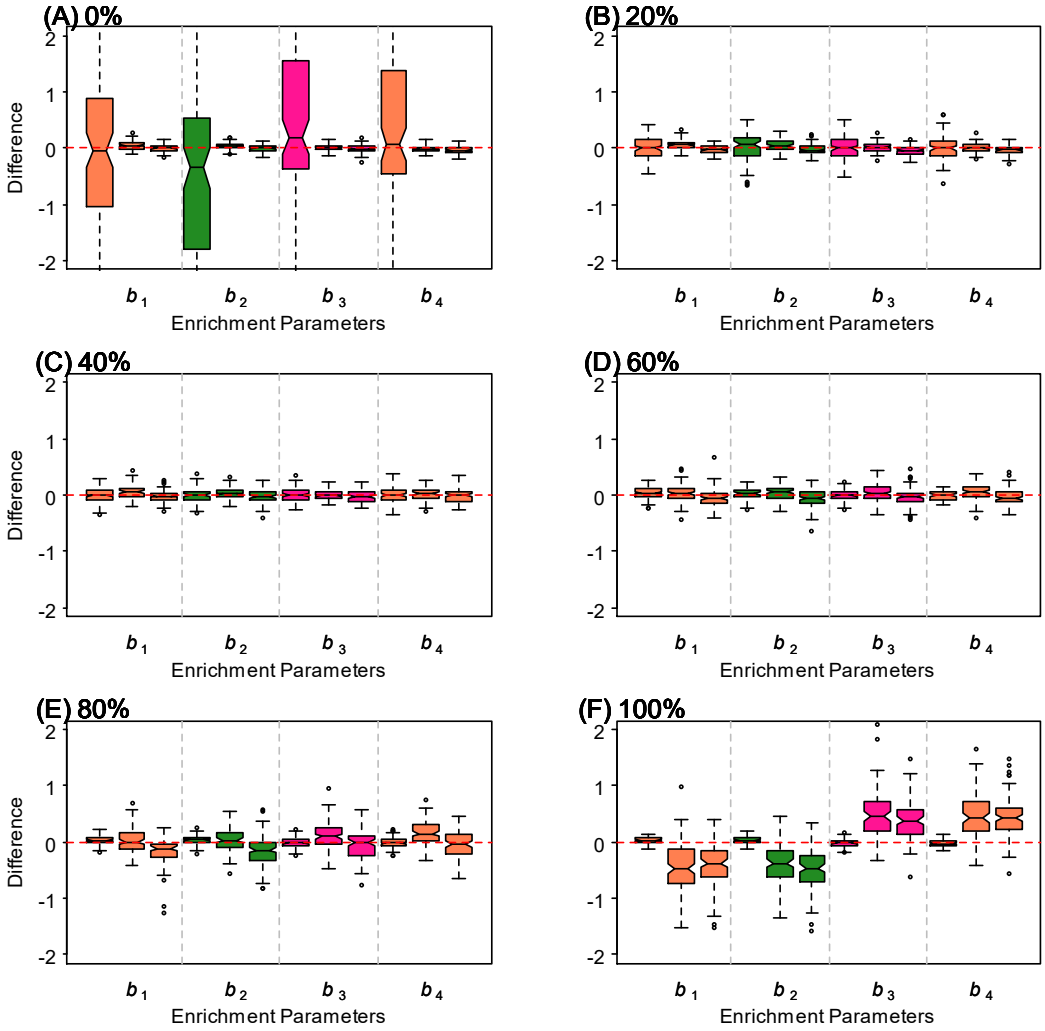

Fig. S12. iMAP is accurate in estimating the enrichment parameters in simulation settings where four informative annotations are present. Sample difference between the estimated values and true values are plotted (y-axis) for four different set of enrichment parameters (x-axis) across 100 simulation replicates. The proportion of pleiotropic causal SNPs considered includes (A) 0%, (B) 20%, (C) 40%, (D) 60%, (E) 80%, and (F) 100%.

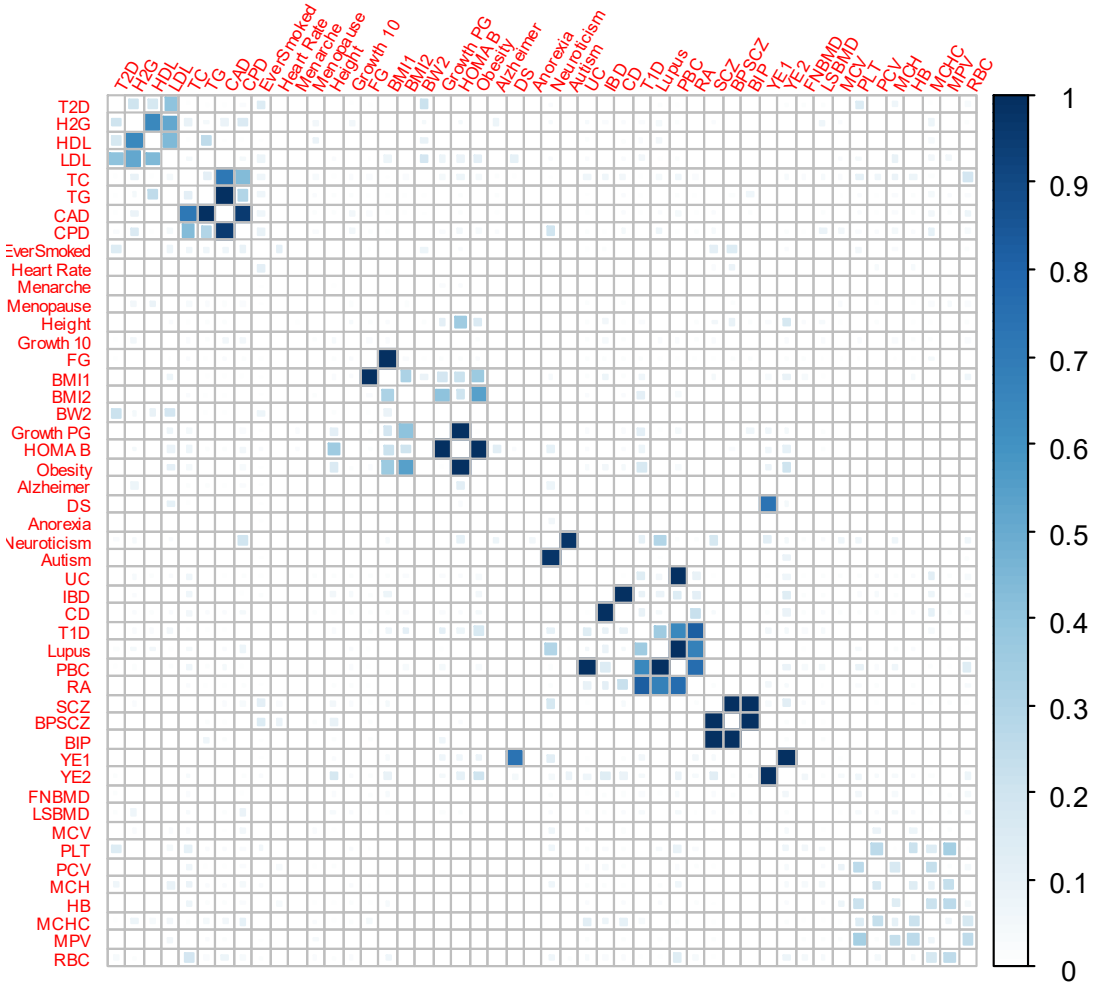

Fig. S13. Proportion of pleiotropic associations ($\pi_{11}/(\pi_{11}+\pi_{10}+\pi_{01})$) for 48 trait pairs in the real data application.

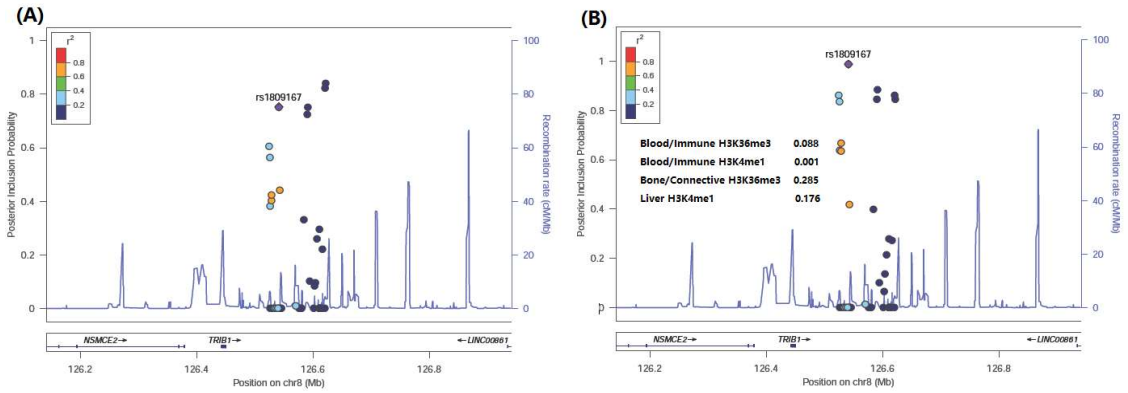

Fig. S14. Locus zoom plots showing a genomic region centered at *rs1809167* near the gene *TRIB1* for the analysis of two traits: high-density lipoproteins (HDL) and triglycerides (TG). The posterior inclusion probability (PIP) by (A) iMAP-naïve and (B) iMAP are shown on the y-axis, which represents evidence for association with both HDL and TG. The selected histone marks along with their enrichment parameter estimates are shown in the Fig. legend.

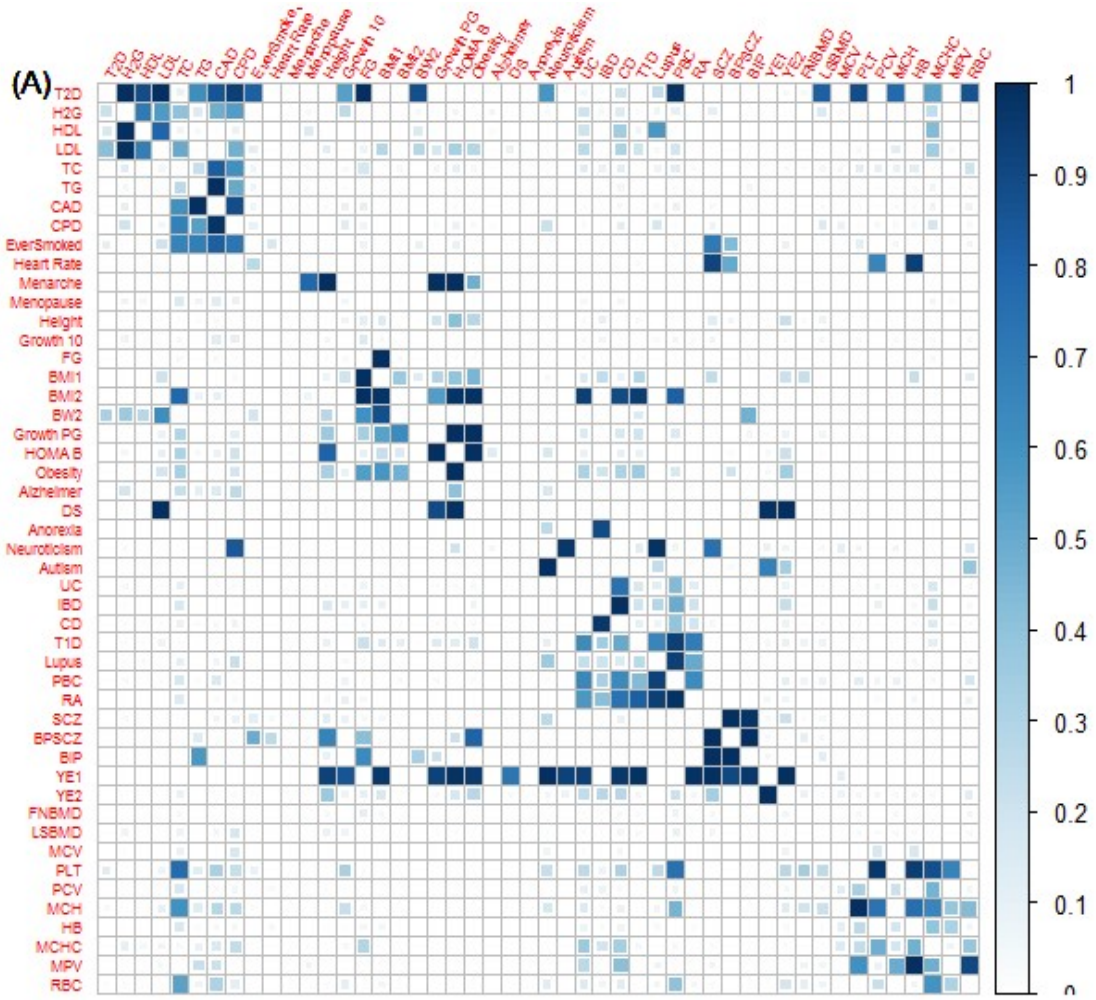
(A)
T2D
H2G
HDL
LDL
TC
TG
CAD
CPD
EverSmoked
Heart Rate
Menarche
Menopause
Height
Growth 10
FG
BMI1
BMI2
BW2
Growth PG
HOMA B
Obesity
Alzheimer
DS
Anorexia
Neuroticism
Autism
UC
IBD
CD
T1D
Lupus
PBC
RA
SCZ
BPSCZ
BIP
YE1
YE2
FNBMD
LSBMD
MCV
PLT
PCV
MCH
HB
MCHC
MPV
RBC
1
0.9
0.8
0.7
0.6
0.5
0.4
0.3
0.2
0.1
0

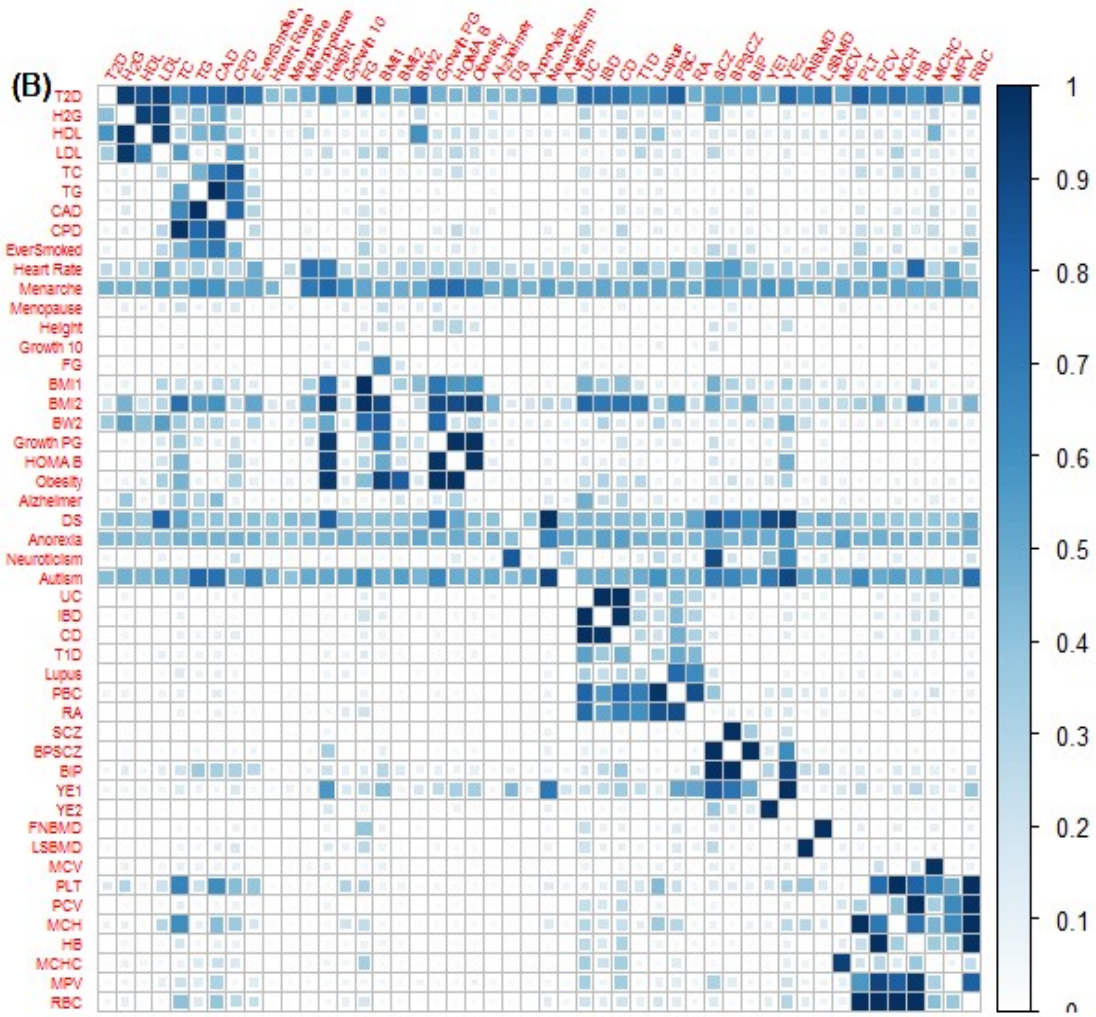
(B)
T2D
H2G
HDL
LDL
TC
TG
CAD
CPD
EverSmoked
Heart Rate
Menarche
Menopause
Height
Growth 10
FG
BMI1
BMI2
BW2
Growth PG
HOMA B
Obesity
Alzheimer
DS
Anorexia
Neuroticism
Autism
UC
IBD
CD
T1D
Lupus
PBC
RA
SCZ
BPSCZ
BIP
YE1
YE2
FNBMD
LSBMD
MCV
PLT
PCV
MCH
HB
MCHC
MPV
RBC
1
0.9
0.8
0.7
0.6
0.5
0.4
0.3
0.2
0.1
0

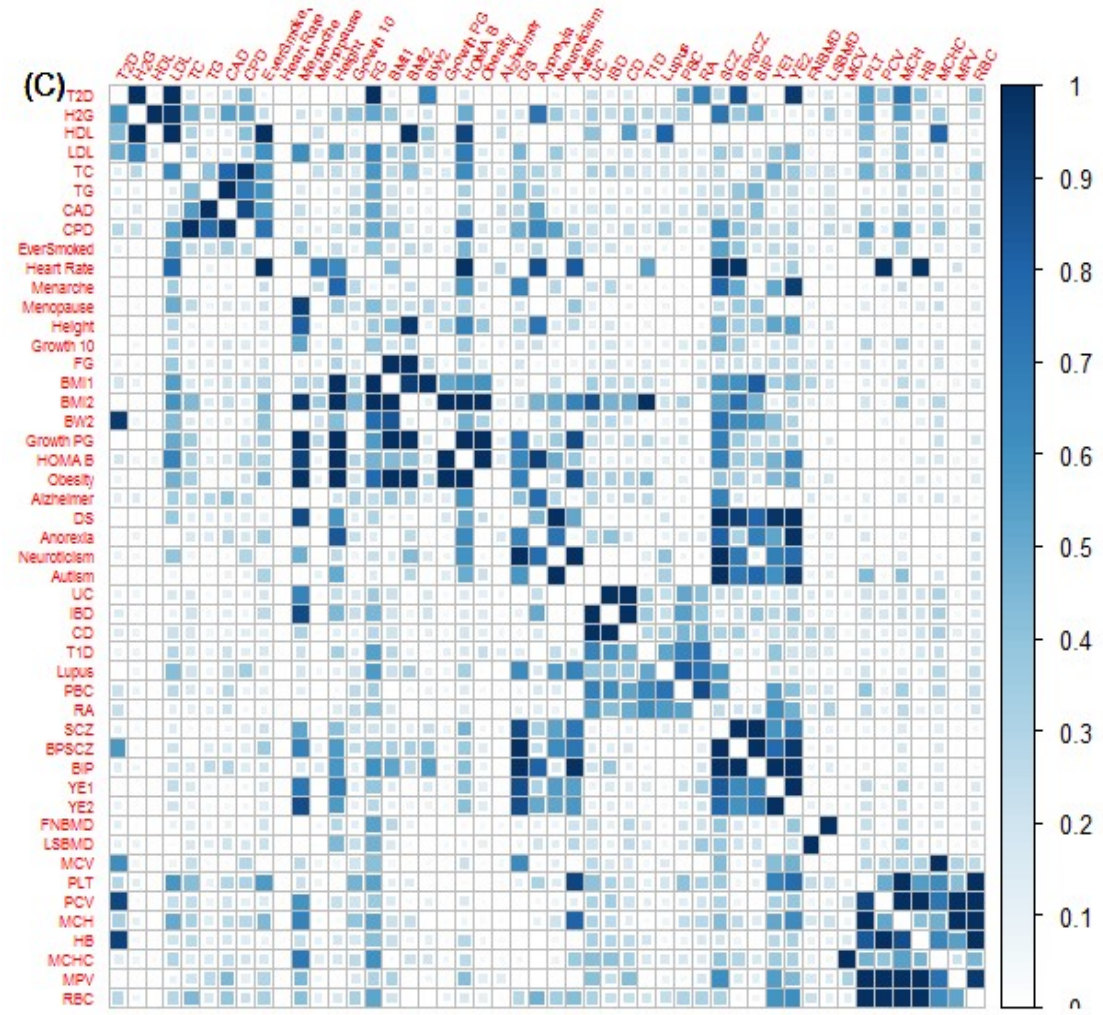

Fig. S15. Estimated probability that a SNP associated with one trait (y-axis) is also associated with the other trait (x-axis), for 48 trait pairs in the real data application. Results are based three different methods that include (A) iMAP-naïve, (B) gwas-pw, and (C) GPA-select.

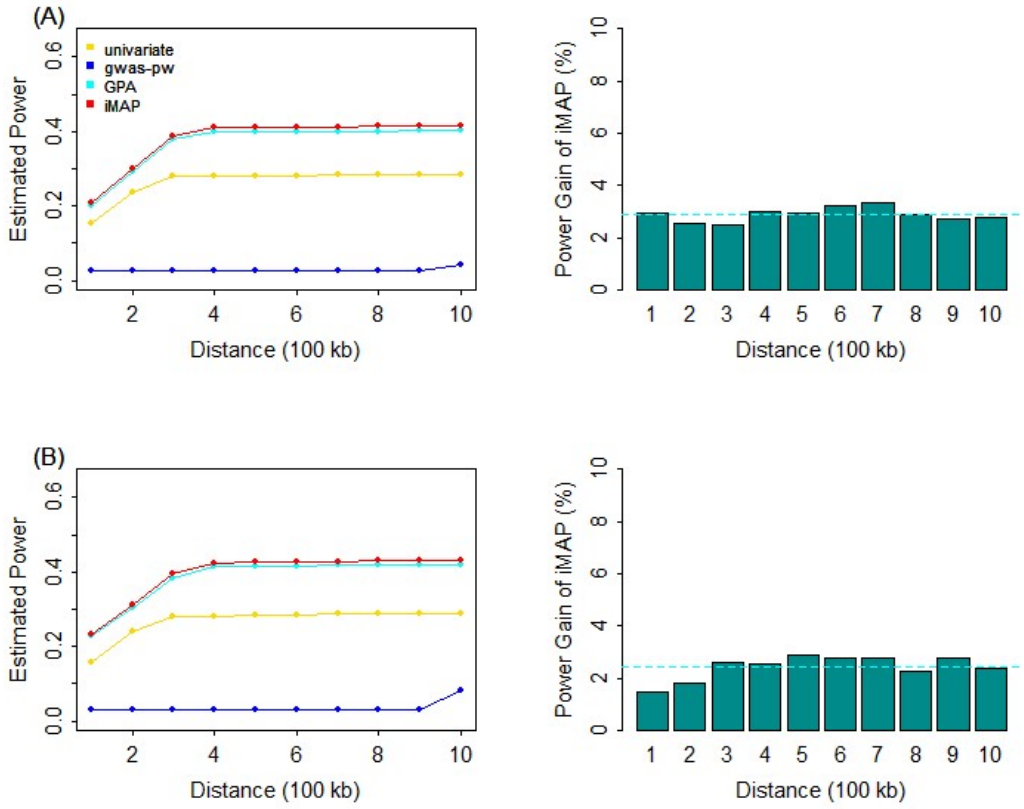
(A)
univariate
gwas-pw
GPA
iMAP
Estimated Power
0.0
0.2
0.4
0.6
2
4
6
8
10
Distance (100 kb)
Power Gain of iMAP (%)
0
2
4
6
8
10
1
2
3
4
5
6
7
8
9
10
Distance (100 kb)
(B)
Estimated Power
0.0
0.2
0.4
0.6
2
4
6
8
10
Distance (100 kb)
Power Gain of iMAP (%)
0
2
4
6
8
10
1
2
3
4
5
6
7
8
9
10
Distance (100 kb)

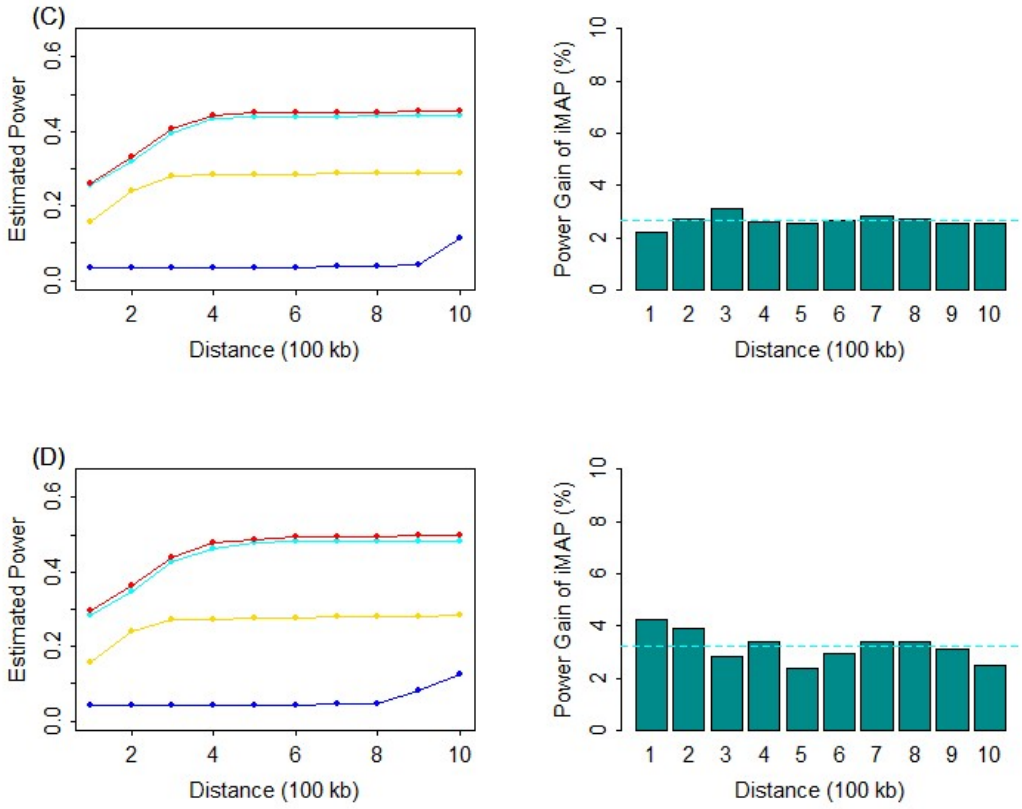
(C)
Estimated Power
0.0
0.2
0.4
0.6
2
4
6
8
10
Distance (100 kb)
Power Gain of iMAP (%)
0
2
4
6
8
10
1
2
3
4
5
6
7
8
9
10
Distance (100 kb)
(D)
Estimated Power
0.0
0.2
0.4
0.6
2
4
6
8
10
Distance (100 kb)
Power Gain of iMAP (%)
0
2
4
6
8
10
1
2
3
4
5
6
7
8
9
10
Distance (100 kb)

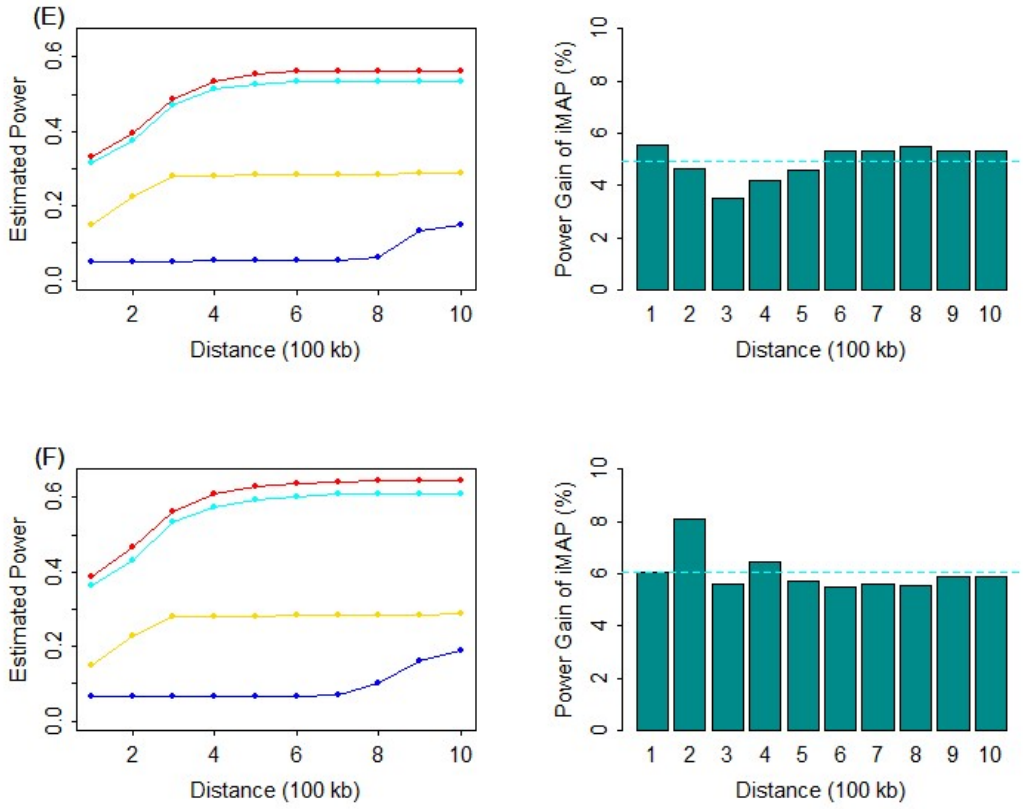

Fig. S16. Power in detecting associated SNPs by various methods in the simulation setting with correlated SNPs. Power (left panels) or power gain brought by iMAP with respect to GPA (right panels) are measured using different distance cutoffs for declaring an association being correct (x-axis). Methods for comparison include univariate analysis (yellow), gwas-pw (blue), GPA (cyan) and iMAP (red). Different panels list results for different proportion of pleiotropic causal SNPs: (A) 0%; (B) 20%; (C) 40%; (D) 60%; (E) 80%; and (F) 100%.

(A)

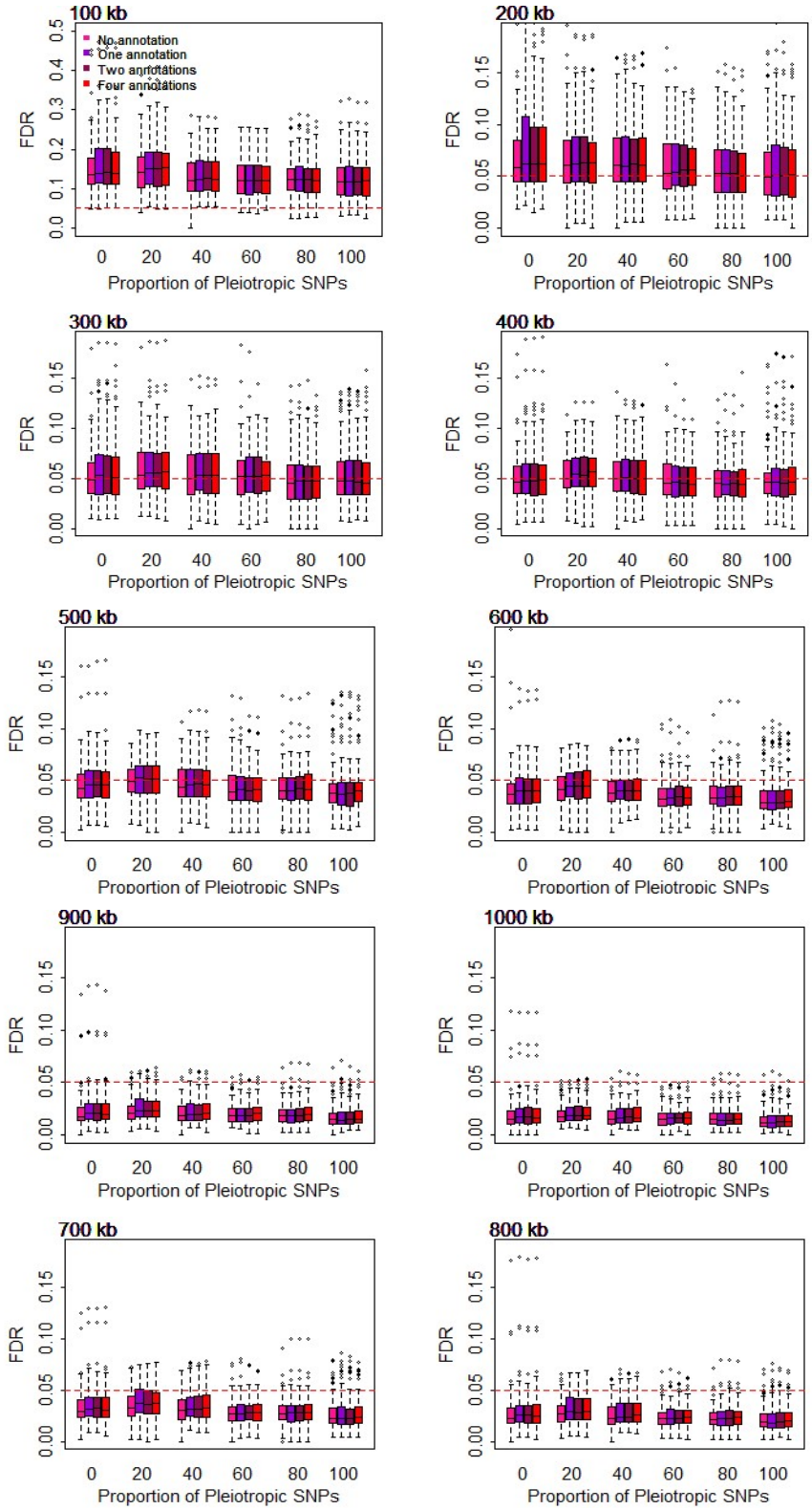
100 kb
200 kb
300 kb
400 kb
500 kb
600 kb
900 kb
1000 kb
700 kb
800 kb
No annotation
One annotation
Two annotations
Four annotations
FDR
Proportion of Pleiotropic SNPs
0
20
40
60
80
100
0.00
0.05
0.10
0.15
0.0
0.1
0.2
0.3
0.4
0.5

(B)

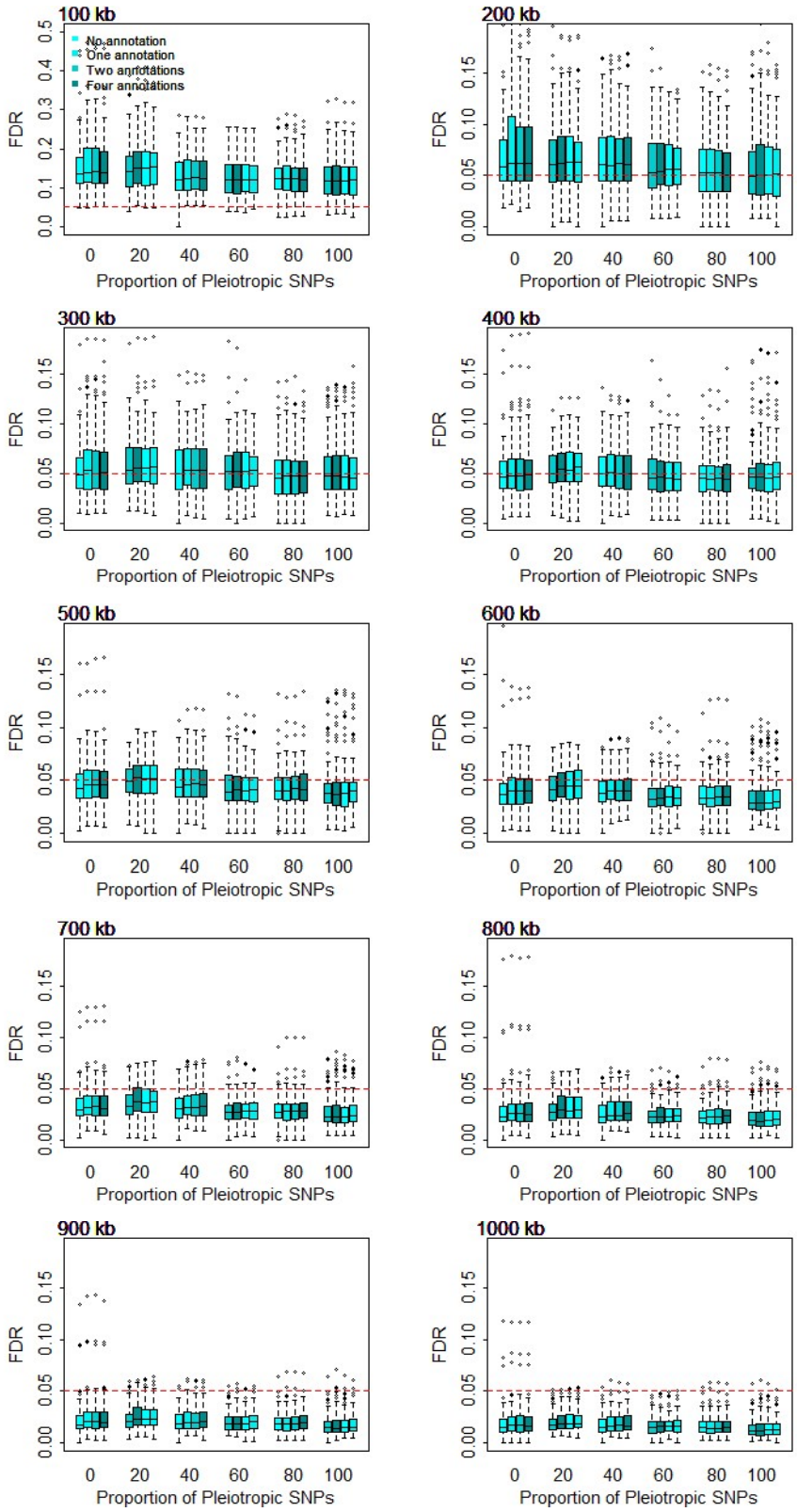
100 kb
No annotation
One annotation
Two annotations
Four annotations
200 kb
300 kb
400 kb
500 kb
600 kb
700 kb
800 kb
900 kb
1000 kb
FDR
Proportion of Pleiotropic SNPs
0
20
40
60
80
100
0.00
0.05
0.10
0.15
0.0
0.1
0.2
0.3
0.4
0.5

(C)

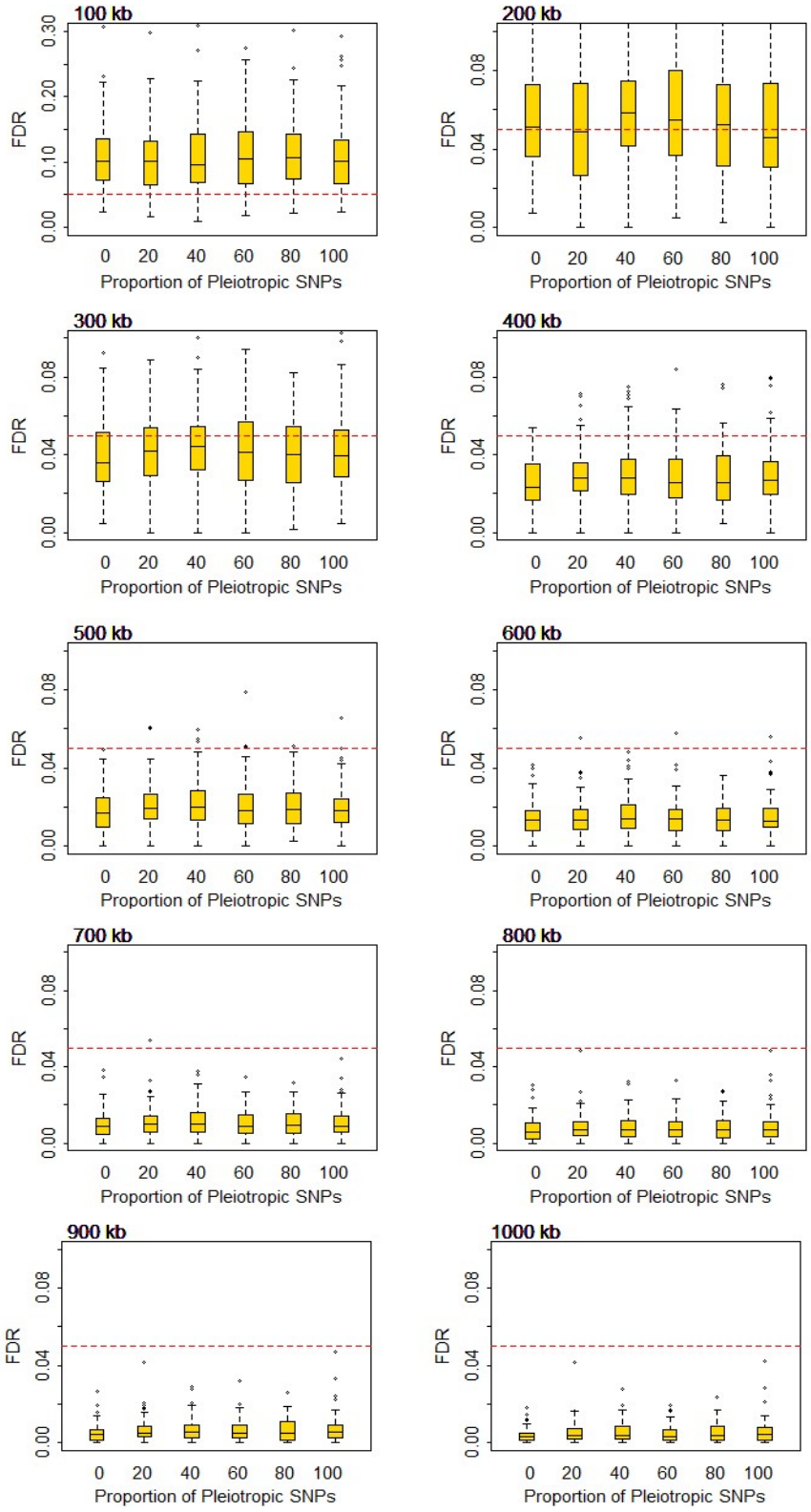
100 kb
200 kb
300 kb
400 kb
500 kb
600 kb
700 kb
800 kb
900 kb
1000 kb
FDR
Proportion of Pleiotropic SNPs
0
20
40
60
80
100
0.00
0.04
0.08
0.10
0.20
0.30

(D)

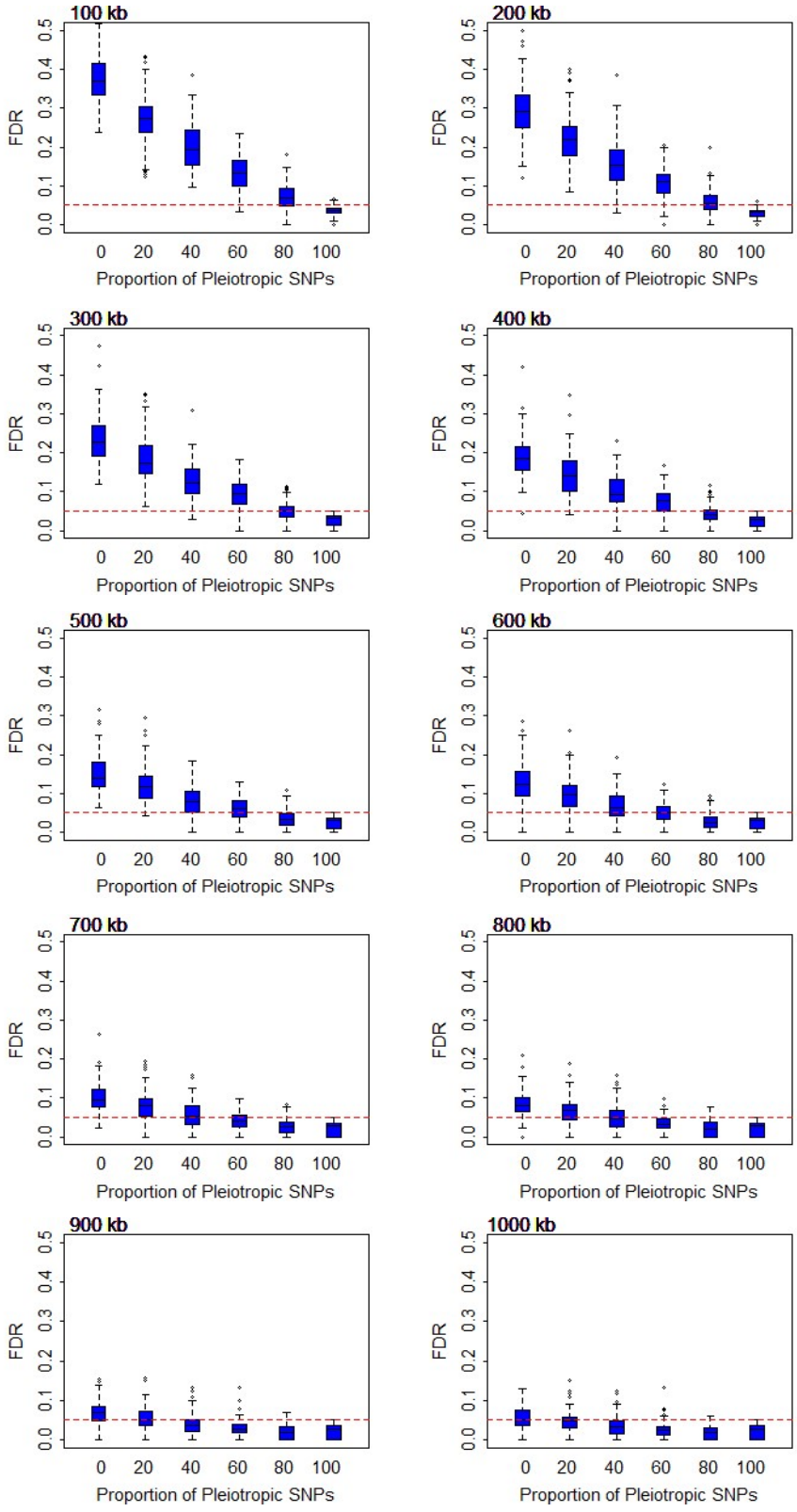
100 kb
200 kb
300 kb
400 kb
500 kb
600 kb
700 kb
800 kb
900 kb
1000 kb
FDR
0.0
0.1
0.2
0.3
0.4
0.5
0
20
40
60
80
100
Proportion of Pleiotropic SNPs

Fig. S17. False discovery rate (FDR) control by various methods in the simulation setting with correlated SNPs. Estimated FDR (y-axis) by (A) iMAP, (B) GPA, (C) univariate analysis, and (D) gwas-pw at the true FDR of 0.05, in settings where the proportion of pleiotropic causal SNPs varies from 0% to 100% (x-axis). The underlying true FDR are computed based on different distance cutoffs for declaring an association being correct (sub-panels).

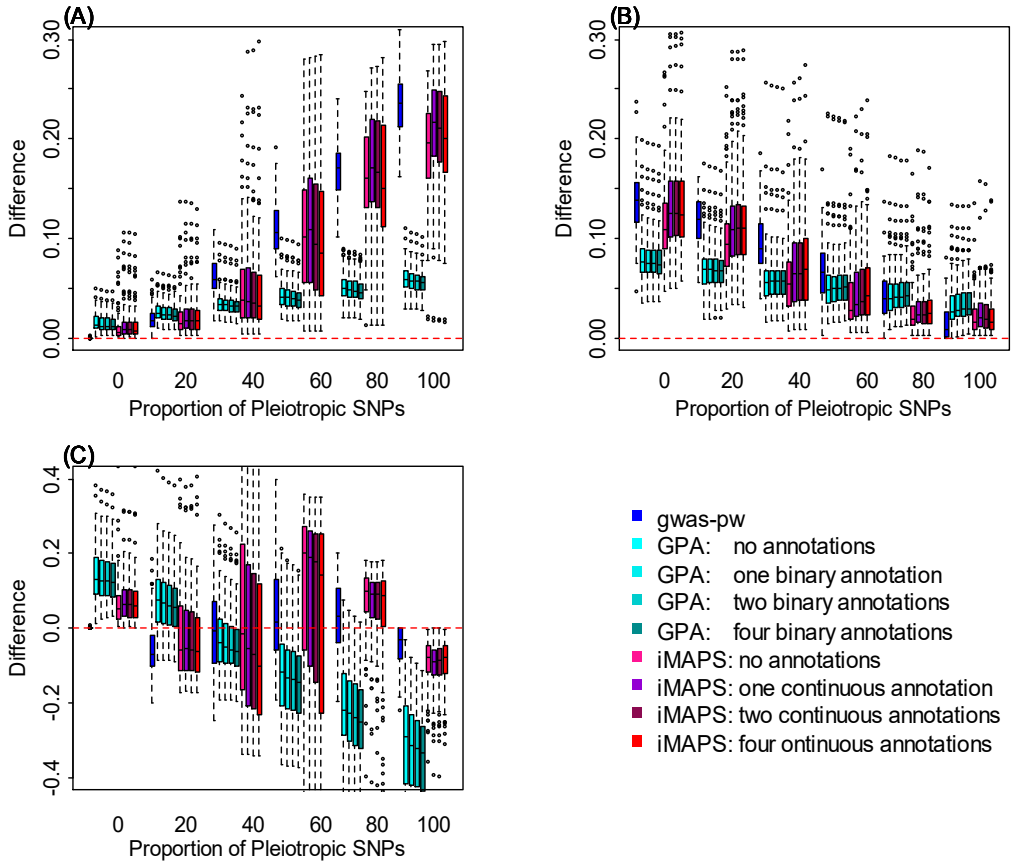

Fig. S18. Estimation accuracy for the proportions of different SNP association categories by different methods in simulations. Methods for comparison include gwas-pw, GPA and iMAP. Four informative annotations are present, so variations of GPA and iMAP that incorporate a different number of annotations (0, 1, 2 and 4) are considered. The difference between the estimated values and truth (y-axis) are computed for various settings where the proportion of pleiotropic causal SNPs varies from 0% to 100% (x-axis). Different quantities of interest are considered: (A) π_{11}, the proportion of SNPs associated with both traits; (B) π_{10}, the proportion of SNPs associated with only the first trait; (C) $\pi_{11}/(\pi_{11}+\pi_{10})$, the proportion of SNPs associated with the first trait that are also associated with the second trait.

Table S1. Information for the summary statistics of 48 traits from 29 GWAS studies

Phenotype	Abbreviation	*n*	h^2	References
Fasting Glucose	FG	46,186	0.074	(Dupuis, et al., 2010)
Height	Height	253,288	0.101	(Wood, et al., 2014)
Body Mass Index	BMI2	122,033	0.050	(Yang, et al., 2012)
2hrGlucose	H2G	15,234	0.053	(Saxena, et al., 2010)
HOMA_B	HOMA B	46,186	0.032	(Dupuis, et al., 2010)
Type 2 Diabetes	T2D	60,786	0.053	(Morris, et al., 2012)
High Density Lipoproteins	HDL	97,749	0.061	(Teslovich, et al., 2010)
Low Density Lipoproteins	LDL	93,354	0.048	(Teslovich, et al., 2010)
Total Cholesterol	TC	100,184	0.058	(Teslovich, et al., 2010)
Triglycerides	TG	94,461	0.068	(Teslovich, et al., 2010)
Coronary Artery Disease	CAD	77,210	0.041	(Schunkert, et al., 2011)
Cigs Per Day	CPD	74,053	0.016	(The Tobacco and Genetics Consortium, 2010)
Ever Smoked	Ever Smoked	74,053	0.037	(The Tobacco and Genetics Consortium, 2010)
Heart Rate	Heart Rate	181,171	0.025	(Den Hoed, et al., 2013)
Menarche	Menarche	182,416	0.062	(Perry, et al., 2014)
Menopause	Menopause	69,360	0.069	(Day, et al., 2015)
Body Mass Index	BMI1	35,668	0.102	(Felix, et al., 2016)
Birth Weight	BW2	26,836	0.056	(Horikoshi, et al., 2013)
Growth 10	Growth 10	13,960	0.236	(Cousminer, et al., 2013)
Growth PG	Growth PG	10,799	0.216	(Cousminer, et al., 2013)
Obesity	Obesity	13,848	0.110	(The Early Growth Genetics Consortium, 2012)
Alzheimer's disease	Alzheimer	54,162	0.045	(Lambert, et al., 2013)
Depressive Symptoms	DS	161,460	0.028	(Okbay, et al., 2016)
Anorexia Nervosa	Anorexia	32,143	0.073	(Boraska, et al., 2014)
Neuroticism	Neuroticism	170,911	0.057	(Okbay, et al., 2016)
Autism	Autism	10,263	0.187	(Cross-Disorder Group of the PGC, 2013)
Ulcerative Colitis	UC	27,432	0.147	(Liu, et al., 2015)

Inflammatory Bowel Disease	IBD	34,652	0.191	(Liu, et al., 2015)
Crohn's Disease	CD	20,883	0.288	(Liu, et al., 2015)
Type 1 Diabetes	T1D	26,890	0.131	(Bradfield, et al., 2011)
Systemic Lupus Erythematosus	Lupus	14,267	0.380	(Bentham, et al., 2015)
Primary Biliary Cirrhosis	PBC	13,239	0.194	(Cordell, et al., 2015)
Rheumatoid Arthritis	RA	37,681	0.094	(Okada, et al., 2014)
Schizophrenia	SCZ	70,100	0.260	(Schizophrenia Consortium, 2014)
Bipolar Disorder/Schizophrenia	BIPSCZ	39,202	0.203	(Ruderfer, et al., 2014)
Bipolar Disorder	BIP	16,731	0.258	(Ruderfer, et al., 2014)
Years of Education	YE1	126,559	0.048	(Rietveld, et al., 2013)
Years of Education	YE2	328,917	0.055	(Okbay, et al., 2016)
FNBMD	FNBMD	32,961	0.084	(Estrada, et al., 2012)
LSBMD	LSBMD	31,800	0.078	(Estrada, et al., 2012)
MCHC	MCHC	56,475	0.033	(Van Der Harst, et al., 2012)
Mean Cell Hemoglobin	MCH	51,711	0.088	(Van Der Harst, et al., 2012)
Hemoglobin Levels	HB	61,155	0.055	(Van Der Harst, et al., 2012)
Mean Red Cell Volume	MCV	58,114	0.092	(Van Der Harst, et al., 2012)
Mean Platelet Volume	MPV	29,755	0.100	(Gieger, et al., 2011)
Packed Cell Volume	PCV	53,089	0.056	(Van Der Harst, et al., 2012)
Platelet Count	PLT	68,102	0.071	(Gieger, et al., 2011)
Red Blood Cell Count	RBC	53,661	0.091	(Van Der Harst, et al., 2012)

Note: The table lists the phenotype name, abbreviation, number of samples, estimates of heritability and references for each of the 48 traits. Growth 10: Height standard deviation score for females at age 10 and males at age 12; Growth PG: Standardized difference in height between age 8 and adult; MCHC: mean corpuscular hemoglobin concentration. Heritability (h^2) is estimated using the LD score regression (Finucane, et al., 2015).

Table S2. Accuracy of iMAP in selecting informative annotations and in estimating the annotation coefficients when ten independent annotations with relatively small effect sizes are present.

Proportion of pleiotropic causal SNPs (%)	True	False	MSE		
			Oracle	Select	Full
0	1.63	0.19	0.08	0.42	9255.47
20	1.23	0.29	0.13	0.91	11574.16
40	1.68	0.23	0.21	0.88	9.75
60	1.75	0.19	0.38	0.89	7.74
80	1.89	0.04	0.14	0.95	19.92
100	2.53	0.08	0.35	3.72	47.03

***Note*:** Simulations were carried out in the presence of ten informative annotations and 100 non-informative annotations for various proportion of pleiotropic causal SNPs (rows). The "True" column lists the number of selected correct non-zero annotation parameters inside the mlogit model. Note that a total of 30 (= 3 × 10) non-zero annotation parameters are expected in the presence of four informative annotations. The "False" column lists the number of selected incorrect non-zero annotation parameters. MSE denotes the median squared error for the estimated annotation parameters across 100 simulation replicates for three different versions of iMAP: the oracle version uses the four informative annotations; the select version performs annotation selection; and the full version includes all annotations without selection.

Table S3. Accuracy of iMAP in selecting informative annotations and in estimating the annotation coefficients for four dependent annotations that have relatively large effect sizes and various correlations.

Proportion of pleiotropic causal SNPs (%)	True	False	MSE		
			Oracle	Select	Full
$r = 0.2$					
0	2.03	0.10	0.04	0.32	7456.87
20	2.20	0.10	0.06	1.77	12032.68
40	3.91	0.22	0.09	0.89	11.13
60	2.98	0.22	0.19	1.37	7.38
80	2.18	0.20	0.45	1.72	18.15
100	2.26	0.21	0.16	3.24	49.86
$r = 0.5$					
0	3.10	0.52	0.05	1.09	9424.40
20	2.86	0.16	0.08	4.09	13239.96
40	4.53	0.45	0.14	2.87	13.37
60	4.37	1.02	0.24	3.29	7.76
80	3.89	1.23	0.68	3.56	16.95
100	3.99	1.54	0.45	5.89	66.75
$r = 0.8$					
0	4.11	2.36	0.13	5.15	12058.61
20	4.38	2.42	0.18	22.53	20981.51
40	6.91	3.92	0.29	16.30	57.28
60	4.51	3.48	0.68	20.56	11.68
80	4.00	3.35	1.68	20.26	21.21
100	4.00	3.52	2.95	25.68	128.54

***Note*:** Simulations were carried out in the presence of four informative annotations (with correlation between x_1 and x_2, x_3 and x_4 varying from 0.2 to 0.8; while x_1, x_2 and x_3, x_4 are independent) and 100 non-informative annotations for various proportion of pleiotropic causal SNPs (rows). The "True" column lists the number of selected correct non-zero annotation parameters inside the mlogit model. Note that a total of 12 (= 3 × 4) non-zero annotation parameters are expected in the presence of four informative annotations. The "False" column lists the number of selected incorrect non-zero annotation parameters. MSE denotes the median squared error for the estimated annotation parameters across 100 simulation replicates for three different versions of iMAP: the oracle version uses the four informative annotations; the select version performs annotation selection; and the full version includes all annotations without selection.

Table S4. Information for the identified loci by iMAP in the joint analysis of HDL and TG

locus	CHR	Genetic Range		Previously Identified Genes	Supporting Reference
		low	up		
1	1	27,013,133	27,285,195	*PIGV, NR0B2*	(Global Lipids Genetics Consortium, 2013)
2	1	39,569,571	40,069,939	*MACF1, PABPC4*	(Surakka, et al., 2015)
3	1	93,651,547	93,817,946	*NR*	*NR*
4	1	109,817,838	109,822,166	*CELSR2, SORT1, PSRC1, SPRT1*	(Chasman, et al., 2009)
5	1	182,054,977	182,200,659	*ANGPTL, ZNF648*	(Surakka, et al., 2015)
6	1	230,291,868	230,324,364	*GALNT2*	(Kathiresan, et al., 2008)
7	2	21,118,983	21,311,691	*APOB*	(Teslovich, et al., 2010)
8	2	85,541,083	85,555,478	*NR*	*NR*
9	2	130,393,136	130,393,136	*NR*	*NR*
10	2	165,501,849	165,558,252	*COBLL1*	(Teslovich, et al., 2010)
11	2	227,034,499	227,181,683	*IRS1*	(Surakka, et al., 2015)
12	3	52,532,118	52,532,118	*STAB1*	(Global Lipids Genetics Consortium, 2013)
13	3	135,932,359	136,272,246	*MSL2L1*	(Global Lipids Genetics Consortium, 2013)
14	4	87,240,799	88,102,967	*AFF1, KLHL8, FAM13A*	(Teslovich, et al., 2010)
15	5	53,297,591	55,857,675	*ARL15*	(Teslovich, et al., 2010
16	6	34,551,086	34,831,866	*SNRPC*	(Surakka, et al., 2015)
17	6	127,432,657	127,437,617	*RSPO3*	(Global Lipids Genetics Consortium, 2013)
18	6	139,828,916	139,840,693	*CITED2*	(Surakka, et al., 2015)
19	7	72,856,269	73,026,378	*TYW1B*	(Teslovich, et al., 2010)
20	7	130,436,459	130,438,214	*KLF14*	(Surakka, et al., 2015)
21	8	9,172,718	10,654,161	*XKR6, PINX1*	(Teslovich, et al., 2010)
22	8	19,564,149	19,928,582	*LPL, RPL30P9*	(Teslovich, et al., 2010)
23	8	116,480,753	116,645,056	*TRPS1*	(Teslovich, et al., 2010)
24	8	126,447,308	126,645,347	*TRIB1*	(Global Lipids Genetics Consortium, 2013)
25	9	15,283,761	15,304,782	*TTC39B*	(Teslovich, et al., 2010)
26	9	107,559,059	107,669,241	*NR*	*NR*
27	10	45,964,505	46,088,061	*MARCH8, ALOX5*	(Global Lipids Genetics Consortium, 2013)

28	10	64,904,071	65,301,725	*JMJD1C*	(Surakka, et al., 2015)
29	10	113,910,721	113,944,271	*GPAM*	(Surakka, et al., 2015)
30	11	10,388,782	10,388,782	*AMPD3, ADM*	(Teslovich, et al., 2010)
31	11	46,701,728	49,675,012	*LRP4, NR1H3*	(Teslovich, et al., 2010)
32	11	61,547,237	65,391,317	*FADS1, FADS2, FADS3*	(Teslovich, et al., 2010)
33	11	116,529,468	117,046,197	*ZNF259, APOA5, ZNF259, APOA1, APOC3, APOA4, BUD13*	(Aulchenko, et al., 2009; Kamatani, et al., 2010)
34	11	122,506,008	122,534,504	*UBASH3B*	(Southam, et al., 2017; Teslovich, et al., 2010)
35	12	57,696,677	57,809,456	*LRP1*	(Global Lipids Genetics Consortium, 2013; Teslovich, et al., 2010)
36	12	123,171,218	125,328,375	*ZNF664, SBNO1, CCDC92, SCARB1*	(Global Lipids Genetics Consortium, 2013; Teslovich, et al., 2010)
37	15	58,552,606	63,439,403	*LIPC*	(Teslovich, et al., 2010)
38	16	56,772,157	57,080,528	*CETP*	(Teslovich, et al., 2010)
39	16	67,605,794	68,428,326	*CTCF, PRMT8M, LCAT*	(Global Lipids Genetics Consortium, 2013; Spracklen, et al., 2017)
40	16	81,514,505	81,519,766	*CMIP*	(Teslovich, et al., 2010)
41	17	37,399,379	38,069,949	*STARD3*	(Teslovich, et al., 2010)
42	17	66,825,940	66,901,366	*ABCA8*	(Teslovich, et al., 2010)
43	17	76,377,482	76,403,984	*SAP30BP*	(Shaffer, et al., 2016)
44	18	47,007,234	47,403,911	*NR*	*NR*
45	18	57,767,635	57,903,604	*NR*	*NR*
46	19	8,469,738	11,347,493	*LDLR*	(Chasman, et al., 2009)
47	19	32,854,470	33,899,065	*PEPD*	Global Lipids Genetics Consortium, 2013; Teslovich, et al., 2010)
48	19	45,449,284	52,324,216	*APOE, APOC1, APOC2, HAS1, LILRA3, LILRB2*	(Teslovich, et al., 2010)
49	20	33,132,364	33,132,364	*NR*	*NR*
50	20	44,483,225	44,643,592	*HNF4A*	(Teslovich, et al., 2010)

51	22	21,922,904	21,983,260	*UBE2L3*	(Spracklen, et al., 2017)

Note: HDL: high-density lipoproteins; TG: triglycerides. A locus is defined as a local genetic region in which the associated SNPs are within 500 kb of each other. Table includes chromosome (CHR), lower and upper base position (low/up) of the locus, nearby genes that were previously identified to be associated with either HDL or TG based on (http://www.ebi.ac.uk/gwas/). *NR*: an associated locus that were not reported previously.

References

Aulchenko, Y.S., *et al.* (2009) Loci influencing lipid levels and coronary heart disease risk in 16 European population cohorts, *Nat. Genet.*, **41**, 47-55.

Bentham, J., *et al.* (2015) Genetic association analyses implicate aberrant regulation of innate and adaptive immunity genes in the pathogenesis of systemic lupus erythematosus, *Nat. Genet.*, **47**, 1457-1464.

Boraska, V., *et al.* (2014) A genome-wide association study of anorexia nervosa, *Mol. Psychiatry*, **19**, 1085-1094.

Bradfield, J.P., *et al.* (2011) A genome-wide meta-analysis of six type 1 diabetes cohorts identifies multiple associated loci, *PLoS Genet.*, **7**, e1002293.

Chasman, D.I., *et al.* (2009) Forty-three loci associated with plasma lipoprotein size, concentration, and cholesterol content in genome-wide analysis, *PLoS Genet.*, **5**.

Cordell, H.J., *et al.* (2015) International genome-wide meta-analysis identifies new primary biliary cirrhosis risk loci and targetable pathogenic pathways, *Nat. Commun.*, **6**, 8019.

Cousminer, D.L., *et al.* (2013) Genome-wide association and longitudinal analyses reveal genetic loci linking pubertal height growth, pubertal timing and childhood adiposity, *Hum. Mol. Genet.*, **22**, 2735-2747.

Cross-Disorder Group of the PGC (2013) Identification of risk loci with shared effects on five major psychiatric disorders: a genome-wide analysis, *The Lancet*, **381**, 1371-1379.

Day, F.R., *et al.* (2015) Large-scale genomic analyses link reproductive aging to hypothalamic signaling, breast cancer susceptibility and BRCA1-mediated DNA repair, *Nat. Genet.*, **47**, 1294-1303.

Den Hoed, M., *et al.* (2013) Identification of heart rate-associated loci and their effects on cardiac conduction and rhythm disorders, *Nat. Genet.*, **45**, 621-631.

Dupuis, J., *et al.* (2010) New genetic loci implicated in fasting glucose homeostasis and their impact on type 2 diabetes risk, *Nat. Genet.*, **42**, 105-116.

Estrada, K., *et al.* (2012) Genome-wide meta-analysis identifies 56 bone mineral density loci and reveals 14 loci associated with risk of fracture, *Nat. Genet.*, **44**, 491-501.

Felix, J.F., *et al.* (2016) Genome-wide association analysis identifies three new susceptibility loci for childhood body mass index, *Hum. Mol. Genet.*, **25**, 389-403.

Finucane, H.K., *et al.* (2015) Partitioning heritability by functional annotation using genome-wide association summary statistics, *Nat. Genet.*, **47**, 1228-1235.

Gieger, C., *et al.* (2011) New gene functions in megakaryopoiesis and platelet formation, *Nature*, **480**, 201-208.

Global Lipids Genetics Consortium (2013) Discovery and refinement of loci associated with lipid levels, *Nat. Genet.*, **45**, 1274-1283.
Horikoshi, M.*, et al.* (2013) New loci associated with birth weight identify genetic links between intrauterine growth and adult height and metabolism, *Nat. Genet.*, **45**, 76-82.
Kamatani, Y.*, et al.* (2010) Genome-wide association study of hematological and biochemical traits in a Japanese population, *Nat. Genet.*, **42**, 210-215.
Kathiresan, S.*, et al.* (2008) Six new loci associated with blood low-density lipoprotein cholesterol, high-density lipoprotein cholesterol or triglycerides in humans, *Nat. Genet.*, **40**, 189-197.
Lambert, J.-C.*, et al.* (2013) Meta-analysis of 74,046 individuals identifies 11 new susceptibility loci for Alzheimer's disease, *Nat. Genet.*, **45**, 1452-1458.
Liu, J.Z.*, et al.* (2015) Association analyses identify 38 susceptibility loci for inflammatory bowel disease and highlight shared genetic risk across populations, *Nat. Genet.*, **47**, 979-986.
Morris, A.P.*, et al.* (2012) Large-scale association analysis provides insights into the genetic architecture and pathophysiology of type 2 diabetes, *Nat. Genet.*, **44**, 981-990.
Okada, Y.*, et al.* (2014) Genetics of rheumatoid arthritis contributes to biology and drug discovery, *Nature*, **506**, 376-381.
Okbay, A.*, et al.* (2016) Genetic variants associated with subjective well-being, depressive symptoms, and neuroticism identified through genome-wide analyses, *Nat. Genet.*, **48**, 624-633.
Perry, J.R.*, et al.* (2014) Parent-of-origin-specific allelic associations among 106 genomic loci for age at menarche, *Nature*, **514**, 92-97.
Rietveld, C.A.*, et al.* (2013) GWAS of 126,559 individuals identifies genetic variants associated with educational attainment, *Science*, **340**, 1467-1471.
Ruderfer, D.M.*, et al.* (2014) Polygenic dissection of diagnosis and clinical dimensions of bipolar disorder and schizophrenia, *Mol. Psychiatry*, **19**, 1017-1024.
Saxena, R.*, et al.* (2010) Genetic variation in GIPR influences the glucose and insulin responses to an oral glucose challenge, *Nat. Genet.*, **42**, 142-148.
Schizophrenia Consortium (2014) Biological insights from 108 schizophrenia-associated genetic loci, *Nature*, **511**, 421-427.
Schunkert, H.*, et al.* (2011) Large-scale association analysis identifies 13 new susceptibility loci for coronary artery disease, *Nat. Genet.*, **43**, 333-338.
Shaffer, J.R.*, et al.* (2016) Genome-wide association study reveals multiple loci influencing normal human facial morphology, *PLoS Genet.*, **12**, e1006149.

Southam, L.*, et al.* (2017) Whole genome sequencing and imputation in isolated populations identify genetic associations with medically-relevant complex traits, *Nat. Commun.*, **8**.
Spracklen, C.N.*, et al.* (2017) Association analyses of East Asian individuals and trans-ancestry analyses with European individuals reveal new loci associated with cholesterol and triglyceride levels, *Hum. Mol. Genet.*, **26**, 1770-1784.
Surakka, I.*, et al.* (2015) The impact of low-frequency and rare variants on lipid levels, *Nat. Genet.*, **47**, 589-597.
Teslovich, T.M.*, et al.* (2010) Biological, clinical and population relevance of 95 loci for blood lipids, *Nature*, **466**, 707-713.
The Early Growth Genetics Consortium (2012) A genome-wide association meta-analysis identifies new childhood obesity loci, *Nat. Genet.*, **44**, 526-531.
The Tobacco and Genetics Consortium (2010) Genome-wide meta-analyses identify multiple loci associated with smoking behavior, *Nat. Genet.*, **42**, 441-447.
Van Der Harst, P.*, et al.* (2012) Seventy-five genetic loci influencing the human red blood cell, *Nature*, **492**, 369-375.
Wood, A.R.*, et al.* (2014) Defining the role of common variation in the genomic and biological architecture of adult human height, *Nat. Genet.*, **46**, 1173-1186.
Yang, J.*, et al.* (2012) FTO genotype is associated with phenotypic variability of body mass index, *Nature*, **490**, 267-272.